the plant journal

The Plant Journal (2020) 104, 979–994 doi: 10.1111/tpj.14975

Differential submergence tolerance between juvenile and adult Arabidopsis plants involves the ANAC017 transcription factor

Liem T. Bui[1], Vinay Shukla[1], Federico M. Giorgi[2], Alice Trivellini[3], Pierdomenico Perata[1], Francesco Licausi[1,2] and Beatrice Giuntoli[1,2,*]

[1]Plantlab, Institute of Life Sciences, Scuola Superiore Sant'Anna, Pisa, Italy,
[2]Pharmacology and Biotechnology Department, University of Bologna, Bologna, Italy, and
[3]Biology Department, University of Pisa, Pisa, Italy

Received 21 February 2020; revised 6 July 2020; accepted 30 July 2020; published online 29 August 2020.
*For correspondence (e-mail beatrice.giuntoli@unipi.it).

SUMMARY

Plants need to attune their stress responses to the ongoing developmental programmes to maximize their efficacy. For instance, successful submergence adaptation is often associated with a delicate balance between saving resources and their expenditure to activate measures that allow stress avoidance or attenuation. We observed a significant decrease in submergence tolerance associated with ageing in *Arabidopsis thaliana*, with a critical step between 2 and 3 weeks of post-germination development. This sensitization to flooding was concomitant with the transition from juvenility to adulthood. Transcriptomic analyses indicated that a group of genes related to abscisic acid and oxidative stress response was more highly expressed in juvenile plants than in adult ones. These genes are induced by the endomembrane tethered transcription factor ANAC017 that was in turn activated by submergence-associated oxidative stress. A combination of molecular, biochemical and genetic analyses showed that these genes are located in genomic regions that move towards a heterochromatic state with adulthood, as marked by lysine 4 trimethylation of histone H3. We concluded that, while the mechanisms of flooding stress perception and signal transduction were unaltered between juvenile and adult phases, the sensitivity that these mechanisms set into action is integrated, via epigenetic regulation, into the developmental programme of the plant.

Keywords: juvenile to adult transition, *Arabidopsis thaliana*, submergence, oxidative stress, hypoxia, chromatin modifications, antimycin A, ANAC017.

INTRODUCTION

Plants go through developmental phases before engaging in reproduction. Such intermediate steps are required to establish offspring production when metabolic resources are amply available, and ensure seed dispersal under convenient environmental conditions. Typically, vegetative development towards full sexual maturation progresses through discrete juvenile and adult stages (Poethig, 2013). The main difference between the two is the competence to integrate endogenous and environmental cues to initiate the next developmental transition: flowering. Often, these phases are marked by distinctive anatomical traits. This can be expressed as extremely divergent dimorphism, originally termed heteroblasty, as in some perennial woody species (Hildebrand, 1875; James and Bell, 2001). In the small annual plant *Arabidopsis thaliana*, the transition between juvenility and adulthood entails the formation of abaxial foliar trichomes, leaf elongation and serration, and a decrease in newly produced cells (Telfer *et al.*, 1997; Tsukaya *et al.*, 2000).

SQUAMOSA PROMOTER BINDING-LIKE PROTEINS (SBP/SPLs) act as conserved integrators between environmental cues, such as photoperiod, and the metabolic state of the plant to drive these morphological changes (Huijser and Schmid, 2011). Active sugar metabolism and carbon availability have been shown to control SPL abundance both at the transcriptional and post-transcriptional level (Matsoukas *et al.*, 2013; Yu *et al.*, 2013). A number of proteins involved in DNA methylation and chromatin remodelling mediate the former layer of regulation, whereas the second is achieved via the microRNAs miR156 and miR157 that cleave and prevent translation of SPL transcripts (Wingler, 2018).

Beyond acting as exogenous cues that promote stage-specific morphological alterations and acquisition of reproductive competence, environmental stresses also exert variable effects on plant life depending on the developmental stage at which they are experienced. This can be explained by the intrinsic tolerance of organs produced at different developmental stages, as well as changes in the response elicited by the perception of the stimulus, as observed in the case of drought, heat and cold stress (Lim *et al.*, 2014; Marias *et al.*, 2017; Kanojia and Dijkwel, 2018). Understanding stress tolerance mechanisms is extremely relevant to efforts to minimize crop yield reduction by adverse environmental conditions. Indeed, several mechanisms that improve plant tolerance and fitness have been identified and are currently exploited (Bechtold and Field, 2018).

Despite the relevant threat to worldwide agricultural production posed by flooding-related events (Voesenek and Bailey-Serres, 2015), the biochemical and molecular bases for tolerance to flooding are less well established than those of the abiotic stress conditions mentioned above. This limitation is connected to the complex nature of the flooding stress itself. First, submergence results in the concomitant depletion of oxygen available for respiration, accumulation of carbon dioxide, ethylene and hydrogen sulphide, and enhanced mobilization of reduced phytotoxic compounds (Bailey-Serres and Colmer, 2014). Following this, once the water level recedes, de-submerged plants are exposed to a dehydration-like stress that jeopardizes their fitness, if not their very survival (Yeung *et al.*, 2019). Flooding tolerance mainly relies on two alternative strategies. The first enables stress avoidance by investing the available resources in rapid elongation and leaf petiole reorientation to emerge from the water surface. The second, instead, reduces ATP and carbohydrate consumption, restraining metabolism to the essential reactions during the stress, to then resume active growth and support reproduction in the aftermath (Loreti *et al.*, 2016). The alternative activation of either strategy is genetically determined, and involves the perception and integration of several cues.

In higher plants, cellular oxygen levels are monitored by the enzymatic class of N-terminal cysteine oxidases of plants (PCOs; Weits *et al.*, 2014; White *et al.*, 2017), which control the activity of the group VII Ethylene Response Factors (ERF-VII; Gibbs *et al.*, 2011; Licausi *et al.*, 2011), key regulators of anaerobic metabolism and the oxidative stress response (Giuntoli and Perata, 2017). The stability of these transcriptional regulators is directly linked to oxygen availability, as under aerobic conditions PCO-catalysed oxidation of an exposed cysteine at their N-terminus by PCO directs them towards degradation via the N-degron pathway (van Dongen and Licausi, 2015). In addition to stabilization of the ERF-VIIs, the accumulation of reactive oxygen species (ROS) and reactive nitrogen species in submergence/hypoxia also leads to the activation of other transcription factors that control the homeostasis of these potentially harmful molecular species, including members of the Heat Shock Factor and NAC families (Gonzali *et al.*, 2015). Recently, this latter family of transcriptional regulators has attracted the attention of the flooding community. A particular subgroup of endoplasmic reticulum (ER)-bound NAC factors can be activated by ROS via endoproteolytic cleavage, whereby the release of N-terminal TF fragments into the nucleus activates genes involved in ROS homeostasis and mitochondrial metabolism (De Clercq *et al.*, 2013; Ng *et al.*, 2013; Meng *et al.*, 2019).

In the present study, we investigate the dependence of Arabidopsis tolerance to flooding conditions on plant age. Having characterized a differential stress response connected with developmental transitions, we propose an ER-tethered NAC TF as a key regulator of the molecular mechanisms behind the phenomenon.

RESULTS

Arabidopsis tolerance to submergence conditions is age dependent

We systematically assessed the flooding tolerance of Arabidopsis plants (Columbia-0 ecotype) at different ages: 2, 3, 4 or 5 weeks after germination, plants corresponding to stage 1.06, 1.12, 3.70 or 3.90 of vegetative development (Boyes, 2001) were subjected to submergence for 2–4 days, with incremental steps of 12 h. Survival was scored 1 week after de-submergence. Two-week-old plants clearly exhibited superior performance under prolonged submergence (Figure 1a) that was further confirmed by their higher survival rates as compared with older plants (Figure 1b).

In an attempt to reduce the space required for the subsequent experiments, we then tested plants grown in pools of equally spaced individuals, in 7-cm pots (Figure 1c), instead of singularly. In these new conditions, 2-week-old plants again displayed better flooding tolerance than 3-week-old ones (Figure 1c,d), demonstrating the suitability of the set-up. In the older plants, advanced signs of stress, such as vitrescence and collapse of leaf tissues, could already be observed at de-submergence (Figure 1c), although loss of survival capacity, in terms of maintenance of leaf production at the shoot apical meristem, was evident only 1 week later.

Attracted by this phenomenon, we decided to investigate its molecular determinants. Our first observation was that the difference between the two phenological stages encompassed the transition from juvenility to adulthood. On average, the rosette of 2-week-old plants consisted of six leaves; 1 week later, this number had doubled (Figure 2a). In this time interval, moreover, canonical markers of adulthood were displayed, such as the appearance of

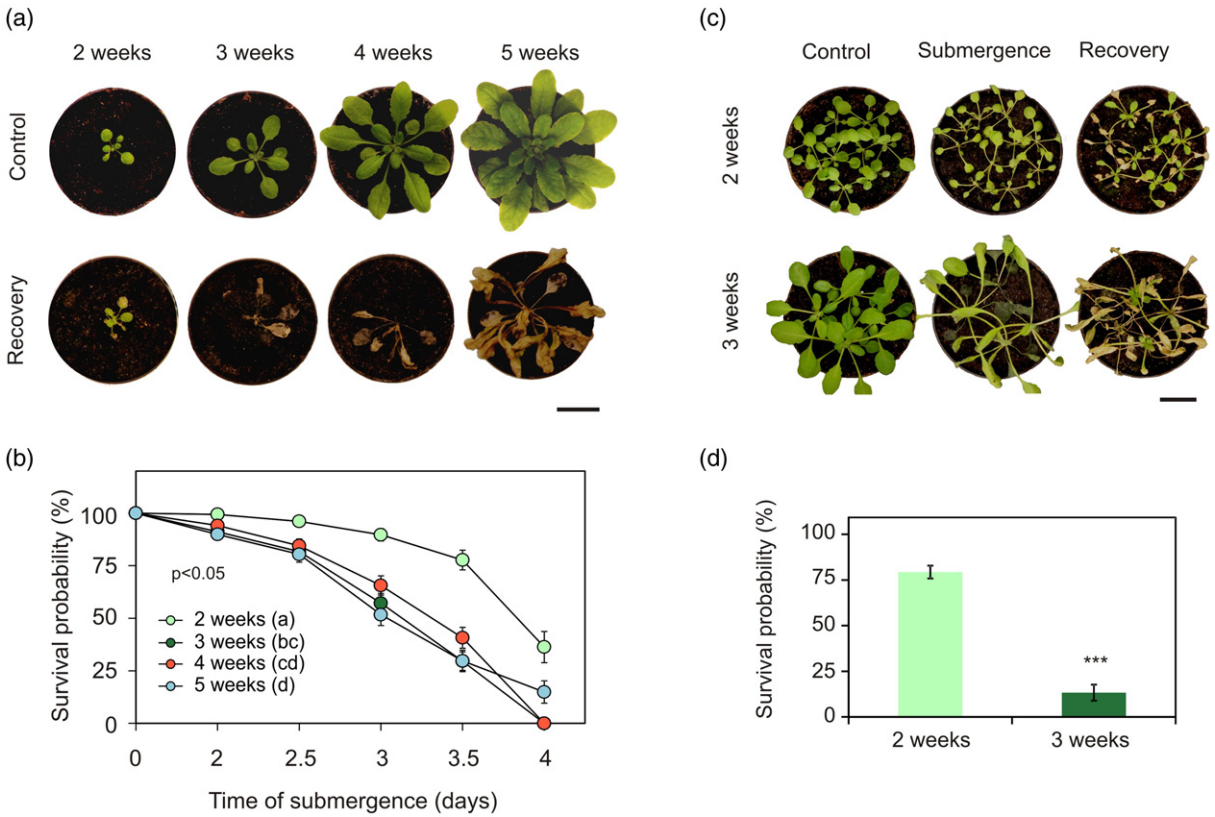

Figure 1. Submergence tolerance of Arabidopsis rosettes at different developmental stages.
(a) Plant phenotypes immediately before the flooding treatment ('Control') and 1 week after recovery following 4 days full submergence ('Recovery'). Scale bar: 2 cm.
(b) Survival probability of Arabidopsis plants at four different ages when subjected to flooding (n = 25 for each combination of plant age and stress duration). Data are mean ± SE from four independent experiments. Letters in brackets indicate statistically significant difference among the survival curves, according to the Kaplan–Meier test ($P < 0.05$).
(c) Phenotypes of 2- and 3-week old plants, grown collectively in pots, before submergence (left), immediately after being de-submerged at the end of a 72-h-long treatment (centre), and 1 week after (right). Scale bar: 2 cm.
(d) Survival rate of plants from (c), scored after 1 week following 72 h submergence (n = 30 for 2 weeks of age, n = 15 for 3 weeks). Data are presented as mean ± SE (n = 4) and asterisks show significant difference according to the Kaplan–Meier test ($P < 0.01$).

trichomes in the abaxial side of the eighth leaf and those subsequently produced, and elongation of leaf shape with serrated margins (Figure 2a).

SPL transcription factors have been identified as crucial regulators of this developmental transition (Huijser and Schmid, 2011; Zhang *et al.*, 2015). A survey of 14 Arabidopsis *SPL* genes in the Genevestigator bioinformatics platform (Hruz *et al.*, 2008) revealed that the respective mRNAs are globally highly expressed in vegetative tissues, and that *SPL3* and *4* mRNAs slightly increase from young to adult plants, by 12% or 19%, respectively (Figure S1). We therefore compared the mRNA levels of a subset of *SPL* genes in shoot tissues of 2- and 3-week-old plants by means of real-time quantitative polymerase chain reaction (qPCR). In our experimental conditions, *SPL3* and *SPL4* mRNA levels showed a significant rise in older plants, while *SPL2*, *5* and *9* showed as expected no detectable fluctuations (Figure 2b). Hence, based on the behaviour of the phase transition markers *SPL3* and *4*, we hereon in refer to 2-week-old plants as juvenile and 3-week-old plants as adult.

The increase of expression of *SPLs* that drives the achievement of adulthood is known to be enabled by suppression of miR156 expression, whereas its overexpression delays the dismissal of juvenile traits. We therefore tested if transgenic plants with ectopic constitutive expression of miR156 also retained higher submergence tolerance. Unexpectedly, 3-week-old *35S:miR156* plants (Wang *et al.*, 2009), characterized by a prolonged juvenile phase, showed higher submergence sensitivity than adult wild-type plants of the same age, both visible at the moment of de-submergence (Figure 2c) and after recovery (Figure 2d). We concluded that ectopic miR156 expression exerted a detrimental effect that overcame the improved tolerance to submergence associated with juvenility.

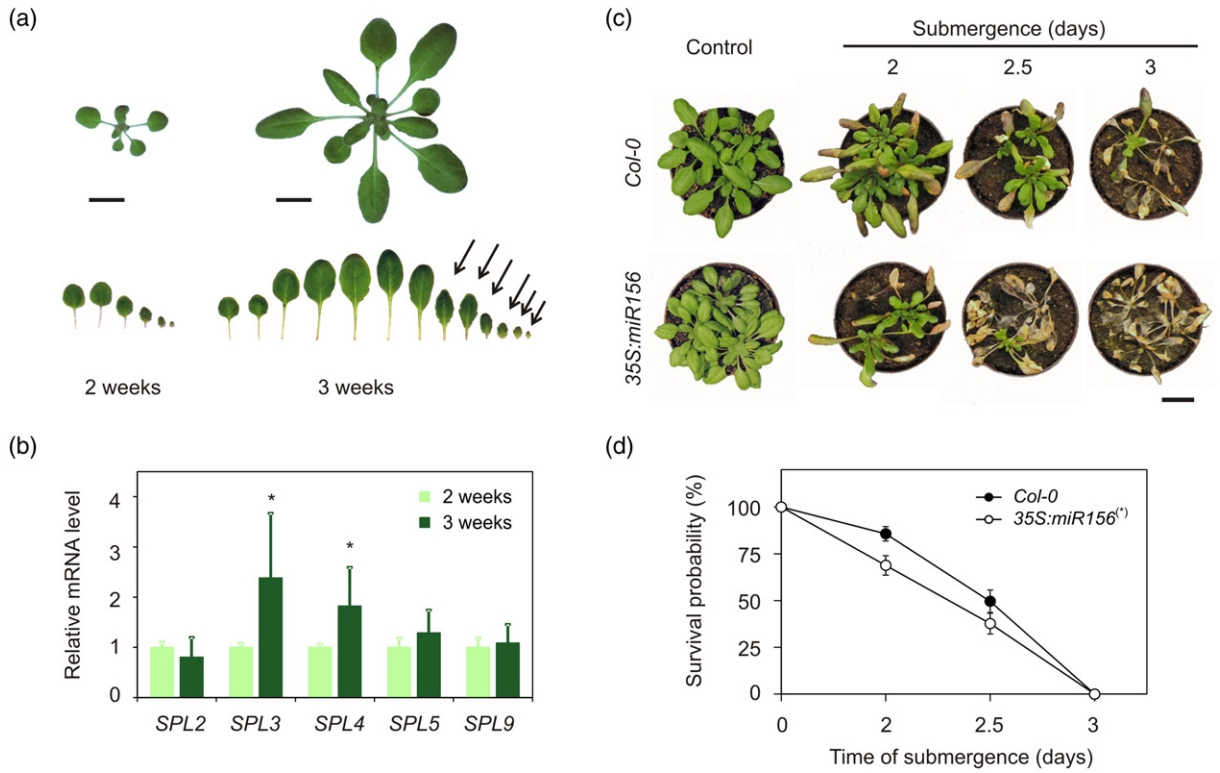

Figure 2. Juvenile to adult phase transition after the second week of growth of Arabidopsis rosettes.
(a) Size and leaf number of 2- and 3-week-old plants. True leaves are displayed progressively according to their age, from left to right. Arrows indicate the leaves with abaxial trichomes, taken as a marker of adulthood. Scale bars: 1 cm.
(b) Relative mRNA level of *SPL2*, *3*, *4*, *5* and *9* genes in 2- and 3-week-old plants as assessed by real-time quantitative polymerase chain reaction (qPCR). Data are mean ± SD, asterisks indicate statistically significant difference at $P < 0.05$ after *t*-test ($n = 4$). Relative expression was set to 1 in 2-week-old plants.
(c) Phenotype in 3-week-old wild-type and *35S:miR156* over-expressors before submergence (left), or immediately after 48, 60 or 72 h of flooding. Scale bar: 2 cm.
(d) Submergence tolerance in the wild-type and *35S:miR156*s ($n = 30$ for each combination of plant age and stress duration), assessed as survival probability. Data are presented as mean ± SE ($n = 4$). The asterisk indicates a significant difference in survival ($P < 0.05$), according to the Kaplan–Meier test.

Molecular responses to hypoxia do not differ between juvenile and adult plants

Having shown evidence against a direct involvement of miR156 in the different tolerance of juvenile and adult plants to flooding, we turned to evaluate whether its molecular bases could be revealed by the expression of marker genes. We analysed a number of markers of anaerobic responses (*ADH, PDC1, Hb1, SAD6, HRA1*), ROS scavenging (*APX1*), and sugar starvation (*DIN6, ATL8, TPS8, KMD4*) in juvenile and adult plants subjected to 12 and 24 h of flooding. Bearing in mind the relevance of both submergence and post-submergence adaptive responses (Yeung *et al.*, 2019), we also collected samples 24 h after de-submergence. Juvenile and adult plants did not exhibit differences in the activation of core low-oxygen-responsive genes, which in plants of both ages were strongly upregulated during flooding and equally abated after 24 h of re-oxygenation (Figure 3; Table S4). Starvation-related genes, instead, exhibited lower expression in juvenile plants after 24 h of submergence as compared with adult plants, but not at the earlier time point (Figure 3; Table S4).

Transcriptome-wide comparison of juvenile and adult plant responses to submergence

Because the targeted analysis did not identify genes that could explain the different flooding tolerance of juvenile and adult plants, we opted for a whole transcriptome approach. Based on our previous tolerance tests, we chose 24 h of dark submergence for the microarray assay, as the longest time point before leaf hyperhydricity could be observed in adult individuals. Plants at the same developmental stages maintained for 24 h under continuous darkness were included as controls. As expected, submergence caused profound rearrangements in plant transcriptomes at both ages: out of ~28 000 genes represented by probe sets in the Arabidopsis Gene 1.0 ST Array platform, 1364 were found significantly up- or downregulated (|

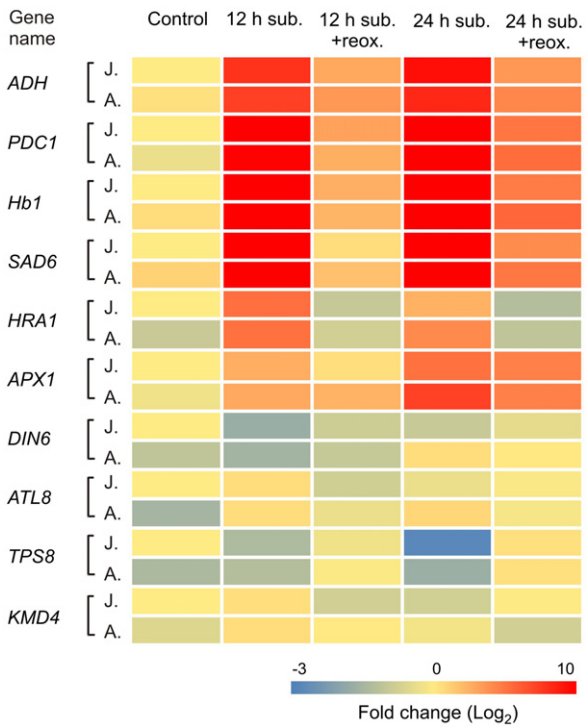

Figure 3. Expression of marker genes for submergence-related processes in treated juvenile or adult plants.
Heatmap representation of relative mRNA levels, assessed by real-time quantitative polymerase chain reaction (qPCR), in juvenile ('J.') or adult plants ('A.'). Transcript abundance was measured after 12 or 24 h of dark submergence, or after 24 h of recovery in fully aerated conditions ('+reox.') following either treatment. Data are mean ± SD ($n = 4$) and are expressed, for each age, as fold change (Log_2 transformed) to the expression in juvenile samples taken immediately before the start of submergence. Supporting values can be found in Table S4. All primers used are listed in Table S1.

$Log_2FC| > 2$, adj. $P < 0.05$) in common in plants from both ages (Figure 4a; Table S5). On the other hand, we found 363 and 232 mRNAs specifically regulated in juvenile or adult plants, respectively (Figure 4a; Table S5). The genes that were significantly differentially expressed at either age were assigned to the Gene Ontology (GO) categories of response to stress, response to hypoxia, response to chemical, response to biotic or abiotic stimuli (Table S6).

We focussed on genes with differential expression in juvenile plants as compared with adult ones under flooding. First, we used real-time qPCR to test a selection of eight genes from those with higher expression in submerged juvenile than adult plants (FC ranging from 1.1 to 4.0, 0.03 < adj. $P < 0.1$; Table S5), to confirm their behaviour. Most of them were indeed significantly more upregulated in juvenile plants as compared with adult ones, after 24 h of submergence, confirming the behaviour revealed by the microarray experiment. In contrast, we could not observe the same trend after 12 h of submergence only (Figure 4b), suggesting that the observed regulation only occurred after long-term submergence.

A stringent selection (adj. $P < 0.05$) of the differentially regulated genes under flooding (hereafter 'ARuS', age-regulated under submergence) retrieved 32 genes that showed significantly higher expression (FC > 2) in submerged juvenile plants and three that were significantly less expressed (FC < −2; Tables 1 and S5). A biclustering analysis of their expression patterns showed clear separation of the 35 genes into two major groups. Moreover, it confirmed their specific regulation by submergence at each age (Figure 4c).

To understand the role of the ARuS genes, we looked at their expression profile and responsiveness in other experimental conditions: a Genevestigator survey over several distinct microarray experiments showed that several of these transcripts respond to abscisic acid (ABA) and antimycin A application, whereas only a few of them were affected by low oxygen stresses (Figure S2; Table S7). Antimycin A is an inhibitor of the mitochondrial electron transport chain, whose application is known to cause a concomitant drop in ATP levels and the production of ROS, similar to what happens under flooding conditions. On the other hand, although drought and ABA-driven response are crucial in the post-submergence phase (Yeung *et al.*, 2018), ABA levels have not been measured in Arabidopsis during submergence, although their ethylene-induced decrease is an integral part of tissue elongation during flooding in different species (Hoffmann-Benning and Kende, 1992; Benschop *et al.*, 2005). Considering our data in the light of the existing literature, we therefore hypothesized that either juvenile plants were able to produce higher ABA and/or ROS levels during flooding, or they were more efficient in eliciting the transcriptional response to such stimuli.

ABA-dependent responses do not contribute to varying submergence tolerance along the vegetative phase change in Arabidopsis

We first focussed on ABA synthesis and signalling, and quantified this stress hormone before and after 12 and 24 h of submergence using an ELISA immunodetection assay. The only observable difference was a higher ABA content in adult plants prior to treatment (Figure 5a). In agreement with previous reports, we then observed a decrease in the level of this hormone upon submergence, which occurred to the same extent at both developmental stages (Figure 5a). These pieces of evidence led us to discard the hypothesis that higher ABA content in juvenile plants could explain the difference in transcriptional response to flooding.

To evaluate whether the juvenile tolerance could arise from enhanced sensitivity to the hormone, we then moved on to compare plant responsiveness to ABA. Using the dedicated Genevestigator tool, we selected five ABA-responsive markers from publicly available experiments:

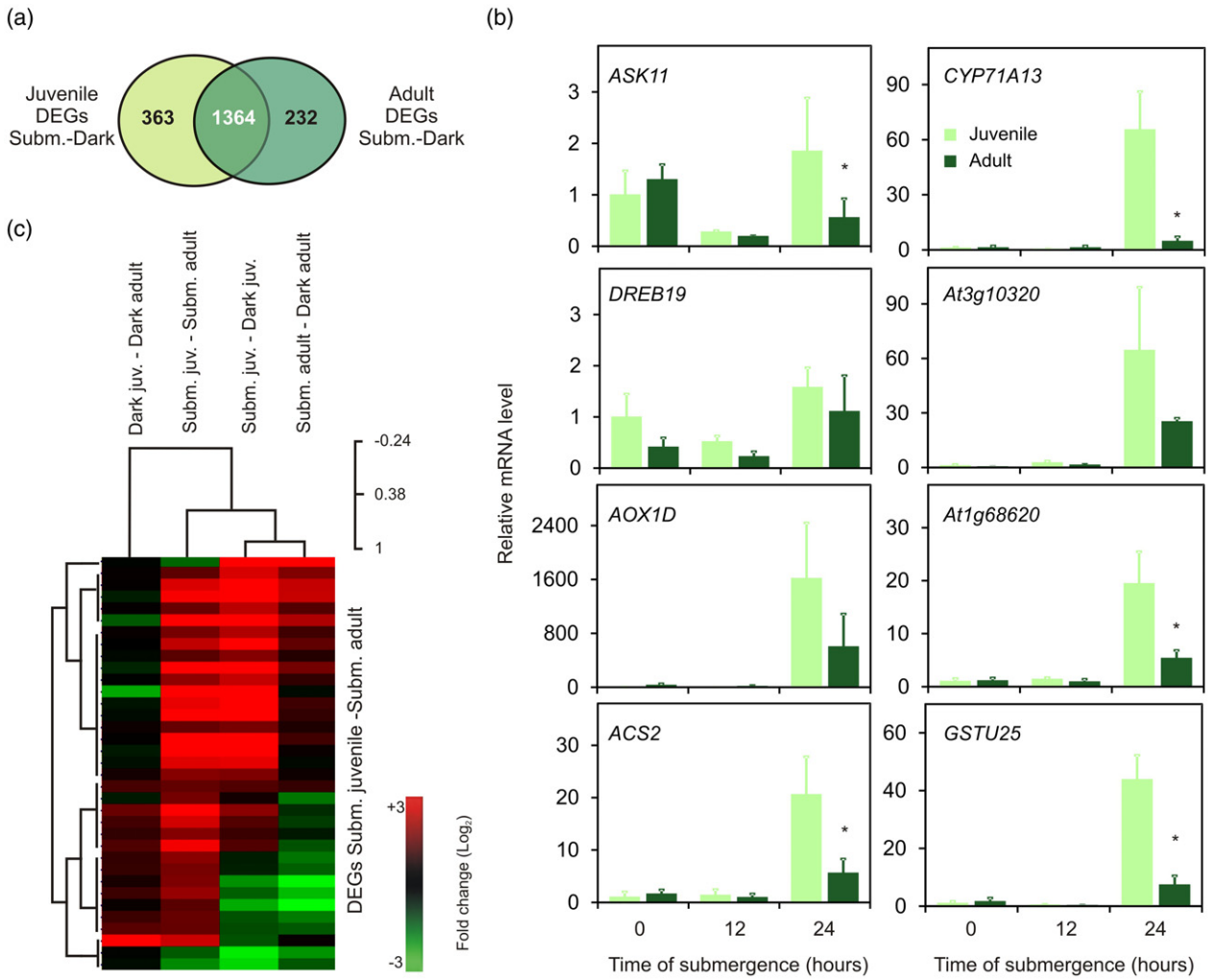

Figure 4. Whole-transcriptome responses of juvenile and adult plants to submergence.
(a) Venn diagram showing all significant differentially expressed genes (DEGs; $|Log_2FC| > 2$, adj. $P < 0.05$) found in the microarray comparison between submergence treated ('Subm.', complete flooding in darkness for 24 h) and control plants ('Dark', 24 h darkness in air) at each stage of vegetative development. FC, fold change.
(b) Relative expression of a subset of the identified stage-specific DEGs upon submergence, validated by means of a real-time quantitative polymerase chain reaction (qPCR) experiment conducted at 12 h and 24 h of submergence. The expression level recorded in juvenile samples at the beginning of submergence ($t = 0$) was set to 1 for each gene. Data are mean ± SD ($n = 4$), asterisks indicate statistically significant difference between adult and juvenile samples at every time point, after *t*-test ($P < 0.05$). The primer used and the gene AGI codes can be found in Table S1.
(c) Heatmap of the significant DEGs ($|Log_2FC| > 1$, adj. $P < 0.05$, stringent selection) between juvenile and adult submergence-treated plants, listed in Table 1. Hierarchical clustering of samples across the four possible microarray comparisons (phylogenetic distances are shown on the top right) and of DEGs (left side) was carried out with Multiple Experiment Viewer (Saeed *et al.*, 2003).

PP2CA (*At3g11410*), *DREB19* (*At2g38340*), the alpha/beta hydrolase *At1g68620*, *AOX1D* (*At1g32350*) and *ACS2* (*At1g01480*). Their expression was analysed by means of qPCR in adult and juvenile plants treated with 10 μM ABA for 3 h. Apart from *ACS2*, which was not induced by the treatment (not shown), the remaining four genes displayed overall higher basal expression and stronger induction by ABA (with the exception of *AOX1D*) in adult plants, suggesting that juvenile plants are not likely to be more sensitive to the hormone under unstressed conditions (Figure 6b). Not only did the more submergence-tolerant juvenile plants not show any differential responses to ABA, but also ABA signalling proved unable to exert a positive impact on flooding tolerance in plants of different ages. Indeed, ABA pre-treatment 3 h before submergence decreased survival probability at both developmental stages (Figure 5c). The results obtained in the analyses described above led us to dismiss the hypothesis of a prominent role by ABA signalling in enhancing tolerance in juvenile plants. On the other hand, these results could suggest that ABA signalling contributes to plant sensitivity to submergence. We tested this by means of *abi2-1* mutant

Table 1 Age-regulated genes under submergence (ARuS) identified from the global transcript analysis

AGI code	Annotation	Log_2FC (Sub2/Sub3)
AT5G55150	Protein of unknown function (DUF295)	4.36
AT1G17180	GSTU25, glutathione S-transferase TAU 25	3.98
AT1G26390	FAD-binding Berberine family protein	3.43
AT5G59330	Bifunctional inhibitor/lipid-transfer protein/seed storage 2S albumin superfamily protein	3.40
AT2G38240	2-oxoglutarate (2OG) and Fe(II)-dependent oxygenase superfamily protein	3.39
AT1G32350	AOX1D, alternative oxidase 1D	3.38
AT3G29250	SDR4, NAD(P)-binding Rossmann-fold superfamily protein	2.99
AT2G04070	MATE efflux family protein	2.93
AT1G55010	PDF1.5, plant defensin 1.5	2.89
AT5G40010	AATP1, AAA-ATPase 1	2.76
AT3G10320	Glycosyltransferase family 61 protein	2.65
AT2G36440	Unknown protein	2.59
AT4G22520	Bifunctional inhibitor/lipid-transfer protein/seed storage 2S albumin superfamily protein	2.51
AT1G70850	MLP34, MLP-like protein 34	2.40
AT5G46960	Plant invertase/pectin methylesterase inhibitor superfamily protein	2.27
AT3G09260	BGLU23, glycosyl hydrolase superfamily protein	1.80
AT2G35730	Heavy metal transport/detoxification superfamily protein	1.71
AT3G53190	Pectin lyase-like superfamily protein	1.64
AT2G23260	UGT84B1, UDP-glucosyl transferase 84B1	1.59
AT2G47010	Unknown protein	1.58
AT1G51140	Basic helix-loop-helix (bHLH) DNA-binding superfamily protein	1.50
AT3G56891	Heavy metal transport/detoxification superfamily protein	1.42
AT4G34160	CYCD3;1, CYCLIN D3;1	1.42
AT4G02290	GH9B13, glycosyl hydrolase 9B13	1.38
AT1G01480	ACS2, 1-amino-cyclopropane-1-carboxylate synthase 2	1.27
AT1G15630	Unknown protein	1.23
AT1G80080	AtRLP17TMM, leucine-rich repeat (LRR) family protein	1.22
AT2G39690	Protein of unknown function (DUF547)	1.20
AT1G07880	ATMPK13, protein kinase superfamily protein	1.18
AT1G61120	TPS4, terpene synthase 4	1.13
AT1G07180	ATNDI1, alternative NAD(P)H dehydrogenase 1	1.06
AT2G32010	CVL1, CVP2 like 1	1.06
AT5G49360	BXL1, beta-xylosidase 1	−1.08
AT5G25180	CYP71B14, cytochrome P450, family 71, subfamily B, polypeptide 14	−1.22
AT1G50040	Protein of unknown function (DUF1005)	−1.63

Genes were filtered for adj. $P < 0.05$.

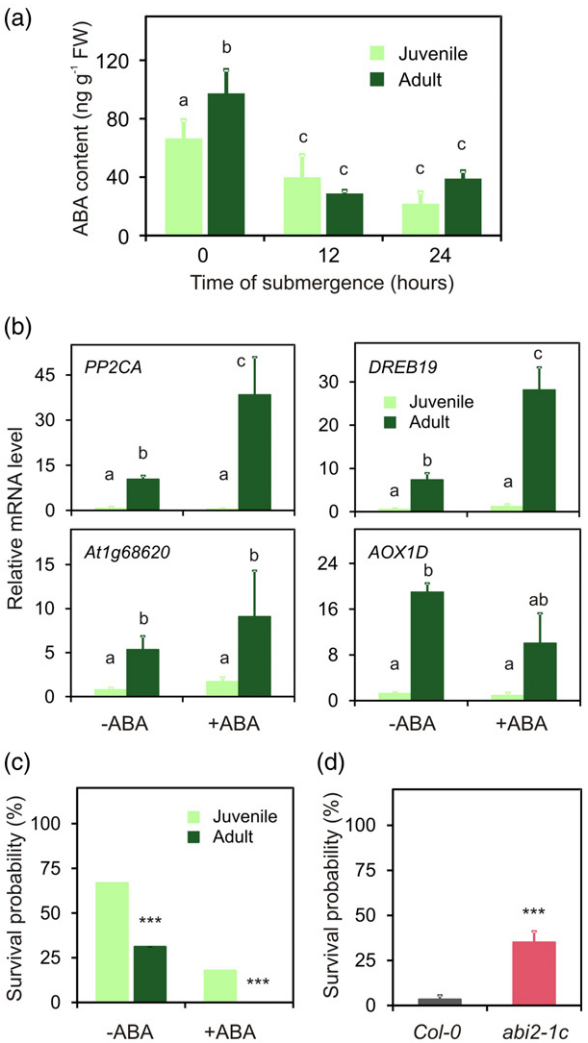

Figure 5. Impact of abscisic acid (ABA) levels and signalling on flooding tolerance across developmental stages.
(a) ABA content in the rosette of 2- and 3-week-old plants at different time points of submergence or prior to treatment. Letters mark statistically significant differences after two-way ANOVA analysis and Holm–Sidak *post hoc* test ($P < 0.05$).
(b) Relative mRNA levels of ABA-responsive genes in juvenile and adult plants treated with 10 μM ABA or water, for 3 h. The expression level recorded in juvenile samples at the beginning of the treatment was set to 1 for each gene. Data are mean ± SD ($n = 4$), different letters indicate statistically significant differences between adult and juvenile samples after two-way ANOVA ($P < 0.05$) and Tukey's *post hoc* test.
(c) Flooding tolerance of juvenile and adult plants treated with 0 or 10 μM ABA 3 h before a 48-h-long submergence.
(d) Tolerance of wild-type and *abi2-1c* adult plants ($n = 15$) subjected to 72 h of dark submergence. Data are presented as mean ± SE ($n = 4$). Asterisks indicate statistically significant differences ($P < 0.01$) as assessed by Kaplan–Meier analysis.

plants, which are ABA insensitive. Indeed, adult *abi2-1* plants displayed significantly better tolerance to submergence than the wild-type (Figure 5d). At this point, determined to pursue the initial question about the differential expression of the identified set of ARuS genes, we moved on to evaluate the contribution of ROS synthesis, perception and downstream signalling.

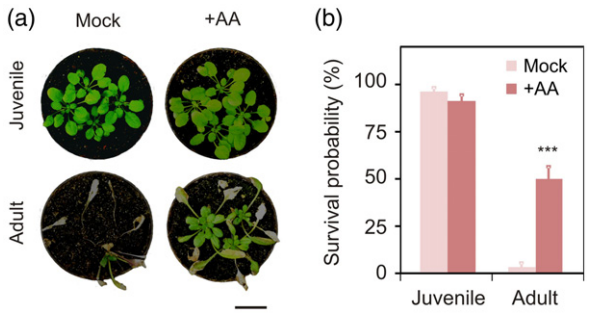

Figure 6. Antimycin A treatment improved submergence tolerance in adult but not in juvenile plants.
(a) Representative phenotype of plants portrayed 1 week after recovery, following dark submergence stress. Plants were sprayed with 100 nM antimycin A (+AA) or 0.001% ethanol solutions ('mock') 6 h prior to 48-h long flooding ('submergence'). Scale bar: 2 cm.
(b) Flooding tolerance of AA-treated plants of both juvenile and adult ages ($n = 20$). Data are presented as mean ± SE ($n = 4$). Asterisks indicate statistical significance at $P < 0.05$ with Kaplan–Meier analysis.

The age-dependent sensitivity to submergence is due to a differential activity of the ROS-regulated transcription factor ANAC017

To substantiate the connection between higher expression of ROS-related genes in juvenile plants (Figure S2b) and better flooding tolerance of plants at this stage, we first tested whether adult plants can be primed to better endure submergence by application of a low dose of antimycin A (100 nM) prior to stress. In this sense, antimycin A pretreatment did indeed prove effective for adult plants, while it did not produce any effect on 2-week old plants (Figure 6a,b). This suggests that promotion of juvenile-upregulated gene expression in older plants can enable them to better cope with flooding conditions.

Higher expression levels of ROS-related genes in juvenile plants might be a consequence of their better ability to activate ROS signalling under submergence, and thereby downstream tolerance strategies, at that stage. However, a qualitative assessment of H_2O_2 accumulation by diaminobenzidine (DAB) staining after 24 h submergence did not show remarkable differences between juvenile and adult plants (Figure S3a); at both ages, ROS production was stimulated by dark submergence and, to a lower extent, by extended prolonged darkness conditions (Figure S3b). Therefore, we favoured the alternative explanation, by which juvenile plants might be especially sensitive to ROS-related signals produced under flooding.

The inhibition of the mETC and consequent ROS production in Arabidopsis has been shown to activate a number of genes involved in the attenuation of oxidative stress by means of a subgroup of NAC transcription factors (Ng *et al.*, 2013). These proteins, which include ANAC013 (At1g32870), 16 (At1g34180) and 17 (At1g34190), are characterized by a transmembrane region at the C-terminus that maintains them in the ER (De Clercq *et al.*, 2013; Ng *et al.*, 2013). Upon oxidative stress, a not-yet identified signal of mitochondrial origin promotes the proteolytic cleavage of the transmembrane domain of ANAC013 and 17 via rhomboid proteases, thereby allowing the cleaved soluble polypeptide to re-localize to the nucleus. We therefore investigated the involvement of these transcription factors in the superior tolerance of juvenile plants to flooding. Within the broad NAC family, by blast analysis we could identify five members with high sequence similarity to ANAC017 and a putative transmembrane region at the C-terminus. ANAC053 (At3g10500) and 78 (At5g04410), which formed a separate clade from ANAC013, 16 and 17 (Figure 7a), have been recently reported to regulate the response to proteotoxic stress (Gladman *et al.*, 2016). Limited to the members of the latter clade, analysis of public gene expression datasets did not show significant differences at the transcriptional level between leaf samples from young or developed plants at the pre-flowering stage (Figure S4). Based on these observations, we decided to focus on ANAC017 as the most highly expressed member of the subgroup in rosette tissues (Figure S4).

When challenged with submergence, a homozygous knockout ANAC017 mutant (*anac017-1*) exhibited significantly lower survival at the juvenile stage, as compared with wild-type plants of the same age (Figure 7b), providing evidence for the involvement of this transcription factor in flooding tolerance. Similar observations were made for ANAC017 mutants at the adult stage (Meng *et al.*, 2020). Although a contribution by ANAC017 homologues to plant performance under submergence cannot be ruled out, the extent of reduction in flooding tolerance we observed in *anac017* supports the hypothesis of a major role of this transcription tolerance in the response of juvenile Arabidopsis plants during the stress. Remarkably, most of the ARuS genes that are responsive to antimycin A appeared to be less upregulated (or sometimes even downregulated) in juvenile *anac017* mutant plants (Figure S2b). A subset of these genes also proved to be less induced upon submergence in juvenile *anac017* plants (Figure S5).

Next, we tested whether ANAC017 is differentially regulated at the post-transcriptional level in juvenile and adult plants. To this purpose, we cloned its full-length coding sequence and fused it to an N-terminal RFP sequence and a C-terminal GFP, which should enable us to follow the fate of the two protein halves subsequently to cleavage (Figure 7c). This construct was transformed in Arabidopsis Col-0 plants under control of the Arabidopsis *UBQ10* promoter. Similar to what has been reported before for different ANAC017 over-expressors (Meng *et al.*, 2019), adult *pUBQ10:RFP-ANAC017-GFP* plants had altered phenotype with shorter petioles and slightly adaxialized leaves at the

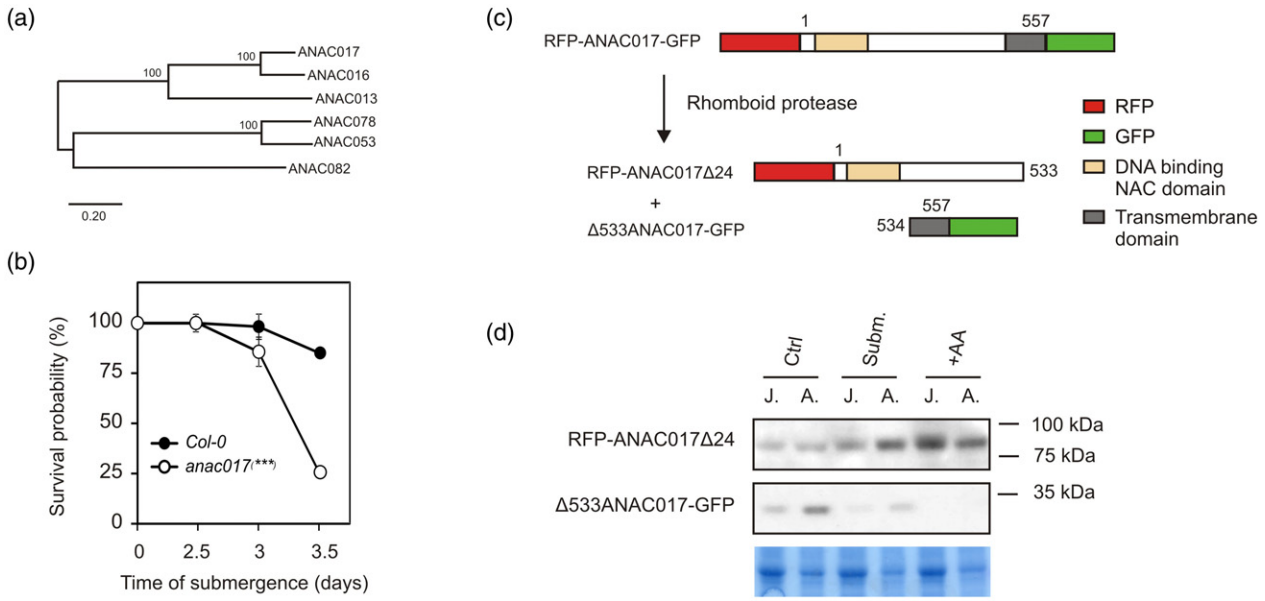

Figure 7. Involvement of ANAC017 in stage-specific responses to flooding.
(a) Phylogenetic relationships among the NAC transcription factor family proteins with highest sequence similarity to the ANAC017 member. Numbers indicate phylogenetic distances calculated with Mega10 with 500 bootstrap value. ANAC082 (At5g09330), a family member lacking any transmembrane domain, was employed in the analysis to root the phylogenetic tree.
(b) Submergence tolerance in 2-week-old *anac017* mutant plants (n = 15), as compared with wild-type. Data are presented as mean ± SE (n = 4). Asterisks indicate significant difference ($P < 0.001$) with Kaplan–Meier analysis.
(c) Schematic representation of a reporter construct for the ANAC017 protein, introduced in plants, and its hypothetical post-transcriptional regulation. In the presence of an oxidative stress, the protein is expected to be cleaved by rhomboid protease family enzymes. In the transgenic plants, the fate of the N-terminal and C-terminal halves can be followed thanks to the RFP and GFP tags fused to the full-length ANAC017 sequence (557 amino acid long), as depicted.
(d) Immunoblotting of juvenile ('J.') or adult plant ('A.') total protein extracts from rosette leaves with either an RFP-specific antibody (above) or a GFP-specific one (below). Plants were kept under submergence ('Subm.') or extended darkness ('Ctrl') for 24 h, or sprayed with 10 μM antimycin A 6 h before harvest. The observed bands match the expected size of an RFP-ANAC017Δ24 peptide (calculated MW≈70 kDa) and a Δ533ANAC017-GFP peptide (calculated MW≈30 kDa). Coomassie staining of the membrane is shown below to visualize protein loading. Full blots are displayed in Figure S7.

adult stage (Figure S6), although they were indistinguishable from the wild-type at the juvenile stage. We investigated ANAC017 cleavage upon mitochondrial stress across the two different developmental stages, in plants experiencing submergence (24 h), extended darkness (24 h) or antimycin A treatment (10 μM, 6 h). Immunodetection of RFP and GFP in total rosette protein extracts showed fragments of about 70 and 30 kDa, respectively, corresponding to the calculated size of the hypothetical cleavage products, RFP-ANAC017Δ24 (retaining an ANAC017$_{1\text{-}533}$ fragment) and Δ533ANAC017-GFP (ANAC017$_{534\text{-}557}$; Figure 7d). In addition to these, the anti-RFP antibody could detect a 35-kDa band, most likely corresponding to an N-terminal fragment of ANAC017, and one about 100 kDa, which we attributed to the uncleaved version of the transcription factor (Figure 7d). The nuclear targeted fragment RFP-ANAC017Δ24 accumulated at higher levels both under flooding and antimycin A treatments than in control conditions, while the ER-localized fragment strongly decreased upon stress treatment independently of the age considered (Figure 7d). Juvenile plants accumulated more RFP-ANAC017Δ24 when treated with antimycin A, but not under submergence. Considered together, these results suggested that different ANAC017 proteolysis upon submergence does not account for the ROS-mediated superior tolerance of juvenile plants.

Stage-specific chromatin modifications occur in vegetative Arabidopsis tissues at age-specific loci

Having excluded the occurrence of transcriptional or post-translational regulation of ANAC017 in the developmental stages under evaluation, we pointed our investigation towards the epigenetic status of the target DNA loci and examined some chromatin modifications in the same selected age-specific genes under submergence described above. To this end, we restrained the analysis to the same set of genes evaluated in Figure 4(b), as interrogation of public datasets confirmed their ANAC017-dependent upregulation in response to mitochondrial stress (Figure 8a). A possible mechanism underlying the differences observed in terms of mRNA accumulation (Figure 4b) might consist of distinct age-specific methylation patterns of the genomic DNA, able to affect RNA polymerase activity. We exploited the methylation-sensitive restriction

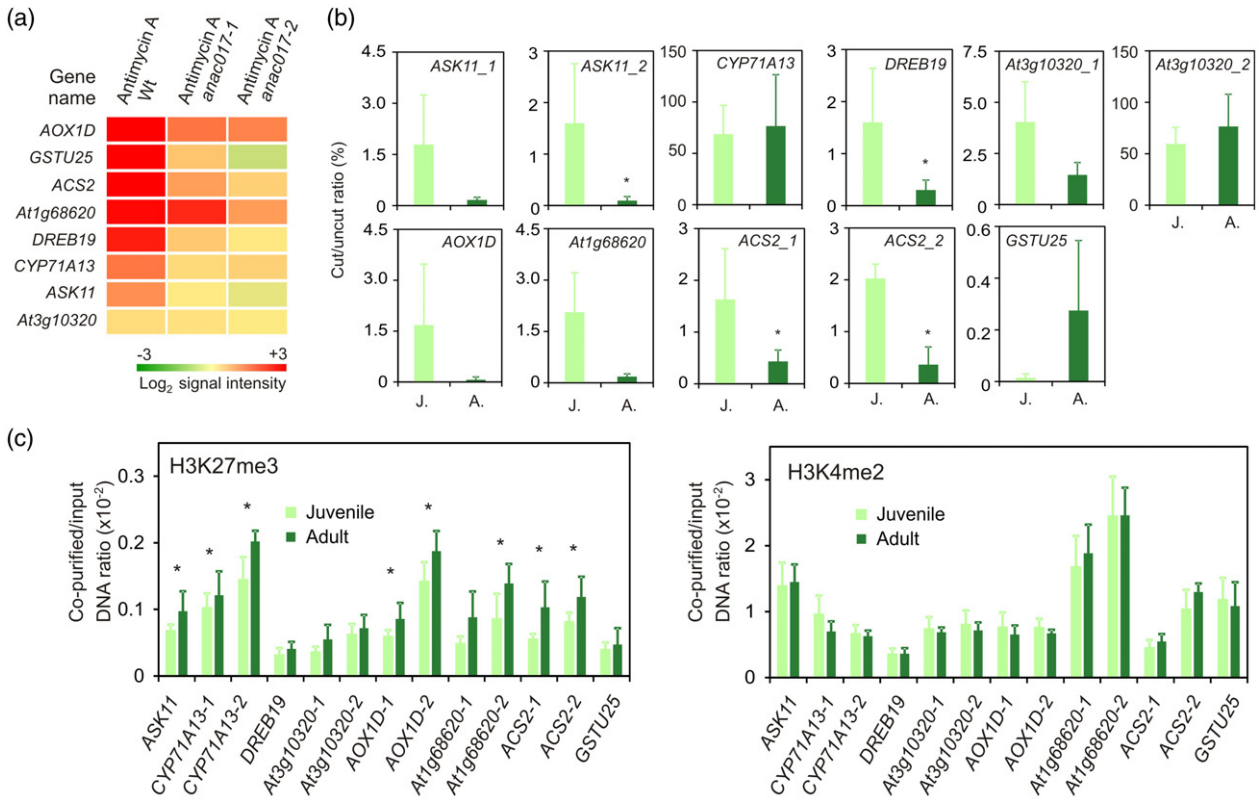

Figure 8. Evaluation of promoter DNA methylation and chromatin accessibility at selected ARuS loci.
(a) Expression patterns of the ARuS genes also shown in Figure 5(b), extracted with Genevestigator from public microarray datasets, showing gene response to antimycin A in two independent *anac017* T-DNA mutant lines and in a background genotype ('Wt'). The datasets used are specified in Table S6. ARuS, age-regulated under submergence.
(b) Methylation-sensitive restriction enzyme-quantitative polymerase chain reaction (MSRE-qPCR) results on the target genes. A higher ratio is suggestive of lower methylation at the target DNA sequence. Genomic DNA extracted from juvenile (J.) or adult (A.) leaf samples was digested using the methylation-sensitive enzymes HspII or SalI, according to the information provided in Table S2, or mock-digested. Cut or uncut DNA was amplified using the primers listed in Table S2. Data are mean ± SD ($n = 4$). Asterisks indicate statistically significant differences after *t*-test ($P < 0.05$).
(c) H3K27 trimethylation and HK4 dimethylation, revealed by chromatin immunoprecipitation (ChIP)-qPCR. Related information can be found in Table S3. Data are mean ± SD ($n = 5$). Asterisks indicate statistically significant differences after *t*-test ($P < 0.05$).

enzyme-qPCR technique (MSRE-qPCR; Hashimoto *et al.*, 2007) to evaluate cytosine methylation of particular HpaII and SalI sites found on the target loci (Table S2). With the exception of *CYP71A13* and *GSTU25*, the analysis revealed a trend for higher methylation of the target loci in juvenile samples (Figure 8b). As control loci for the analysis, we used the housekeeping gene *UBQ10* and, based on the results in Figure 2(b), *SPL9*, whose chromatin was not supposed to be differentially accessible in plants of different ages; in both cases, DNA methylation at the selected sites resulted to be unchanged (Figure S8).

In another scenario, juvenile and adult plants might differ in terms of chromatin accessibility to ANAC017, after its activation by mitochondrial stress signalling, as well as to other regulatory factors. We thus analysed a histone 3 modification known to play a repressive role, K27 trimethylation (H3K27me3), and found that five of the gene promoters evaluated, namely *ASK11*, *CYP71A13*, *AOX1D*, *At1g68620* and *ACS2*, showed significantly higher enrichment in adult plants in comparison with juvenile ones, in at least one analysed region (Figure 8c). This observation hints at a lower extent of chromatin repression at the target loci in juvenile plants, which might facilitate the induction of such genes upon the onset of submergence. In contrast, a second epigenetic marker of repression, H3K4 dimethylation (H3K4me2; Liu *et al.*, 2019), showed no significant differences in our conditions (Figure 8c).

DISCUSSION

Plants, including Arabidopsis, shift through developmental phases integrating cues from the environment and by modulating genetic programmes. To the best of our knowledge, this study represents the first attempt to investigate submergence tolerance in Arabidopsis at different stages of plant growth. We consistently observed higher tolerance of juvenile plants in comparison to older ones (Figures 1 and 2). The transition from juvenility to adulthood is accompanied by an increase in the level of SPL proteins. Inversely, the

elevation of SPL protein correlates with the downregulation of the miR156 transcript, which acts as a negative regulator of *SPL* genes (Wu *et al.*, 2009; Huijser and Schmid, 2011). Here, we confirmed that adult plants increase significantly the expression of *SPL3* and *SPL4* as compared with juvenile plants (Figure 2b). This is in agreement with that reported previously, when plants were grown under long- and short-photoperiodic conditions (Xu *et al.*, 2016). In neutral photoperiods, we could instead not measure the upregulation of other *SPL* genes (such as *SPL2* and *SPL9*) whose products have been functionally associated with vegetative phase changes, suggesting that *SPL3* and *SPL4* may be involved in the regulation of other, less obvious, aspects of the juvenile-to-adult phase transition. Surprisingly, however, artificial procrastination of adulthood by miR156 overexpression did not improve tolerance to submergence (Figure 3c,d), indicating that either parallel signalling pathways, associated with juvenility to adulthood transition, are responsible for this phenomenon, or that ectopic expression of the miRNA impaired the plant's ability to respond to flooding.

The molecular response to submergence broadly overlapped between juvenile and adult plants, and corresponded to the one that we previously reported for 4-week-old plants (Giuntoli and Perata, 2017). The typical hypoxia-marker genes were strongly induced after 12 and 24 h of submergence, as well as transcripts coding for proteins related to ROS homeostasis, protein stabilization and defence mechanisms (Figure 3). Juvenile plants exhibited faster and stronger induction of *ADH*, suggestive of enhanced fermentation, while adult plants showed the highest induction of starvation-related genes *DIN6* and *TPS8*. Repression of some starvation-associated genes under submergence has been reported before (Lee *et al.*, 2011), and is believed to take part to the quiescence response strategy that is typical of Arabidopsis. A differential regulation of starvation-related genes was expected, as carbon availability has been shown to affect survival to submergence in Arabidopsis by modulating the magnitude with which ERF-VII transcription factors regulate the expression of fermentative genes (Loreti *et al.*, 2018). Indeed, juvenile plants have smaller leaves than adult ones, with higher carbon reserves, including sucrose and soluble sugars (Durand *et al.*, 2018). Thus, we speculate that the superior tolerance to submergence in juvenile plants is associated with the promptness and extent of the metabolic and molecular responses activated at this stage.

Under submergence conditions, the amount of transcripts identified as differentially expressed between juvenile and adult individuals ('ARuS' genes) was relatively small (Table 1). Several of them have been reported to respond to treatments that produce ROS or activate the ABA signalling pathway. A real-time qPCR survey, carried out on a subset of these genes, revealed that they are upregulated after 24 h but not 12 h of submergence, indicating that this response is activated late during submergence (Figure 4b).

Abscisic acid has been investigated as a hormone potentially involved in submergence responses in several plant species, including both dicots and monocots (Hook *et al.*, 1988; Hoson *et al.*, 1993; Hurng *et al.*, 1994; Lee *et al.*, 2009). Consistent with previous reports, our data confirmed that ABA levels decreased upon submergence at both developmental stages (Figure 5a). Adult plants showed stronger ABA responsiveness under non-flooded conditions (Figure 5b), suggesting that other signals beyond ABA are involved in the upregulation of the subset of ARuS genes under submergence. ABA is actually more likely to play a negative role in the adaptation of plants to submergence, as ABA pre-treatment reduced submergence survival at both ages (Figure 5c). Accordingly, an ABA-insensitive mutant (*abi2-1*) exhibited increased flooding tolerance in adult plants (Figure 5d). Taken together, our data point at ABA signalling as a determinant of plant sensitivity to submergence, and exclude that increased ABA levels or responsiveness contributed to superior tolerance to submergence in juvenile Arabidopsis plants.

On the other hand, we could link this feature to the impairment of mitochondrial activity. A meta-analysis (Figure S2b) indicated that one-third of the ARuS genes could be also upregulated by treating plants with antimycin A, which inhibits mtETC complex III and consequently leads to the production of ROS. These genes were mainly genes related to ROS homeostasis, mitochondrial functioning and cell wall remodelling, which potentially improve survival under stress conditions. Indeed, pre-treatment of adult plants with antimycin A significantly improved flooding survival in adult plants but not juvenile ones. We speculated that either plants at the juvenile stage are especially sensitive to ROS-related signals produced under submergence conditions, or that they are more promptly able to produce this signal when the stress occurs. We could not detect differences between juvenile and adult plants after DAB staining for hydrogen peroxide under control or stress conditions (Figure S3). Alternatively, the application of antimycin A might have promoted a quiescence strategy that would be beneficial to adult plants. As adult plants showed higher expression of some starvation marker genes (Figure 3) than juvenile plants, limiting their respiration through chemical inhibition of the mETC might restrain sugar consumption and thereby reduce the amount of experienced carbon starvation. As observed above, perception of low sugar availability has been reported to restrain the induction of anaerobic genes in submerged plants, generating a mechanism that contributes to a quiescence response strategy in Arabidopsis (Loreti *et al.*, 2018). Future investigation is needed to clarify whether supplementation of antimycin A could be effective in triggering this kind of metabolic adaptation during submergence.

A group of ER-bound NAC transcription factors has been reported as main regulators to the nuclear response to mitochondrial dysfunction (De Clercq *et al.*, 2013; Ng *et al.*, 2013; Meng *et al.*, 2019). Mitochondrial ROS production has been proposed to lead to the release of N-terminal fragments of these factors, by action of rhomboid proteases, into the nucleus, where they act as transcriptional regulators. Among them, ANAC017 was abundantly expressed in both juvenile and adult plants (Figure S4), and T-DNA-mediated inactivation of *ANAC017* significantly reduced survival under submergence conditions compared with the wild-type (Figure 7b). By exploiting dual fluorescent tagging of the protein (Figure 7c), we observed constitutive endoproteolytic cleavage of ANAC017 under control conditions at both developmental stages considered (Figure 7d). We also observed accumulation of the N-terminal fragment in the case of submergence and antimycin A treatment, while the C-terminal fragment decreased after both treatments (Figure 7d). This observation would invoke additional proteostatic mechanisms acting upon this transcription factor after its proteolytic cleavage. In addition, ANAC017 transgenic plants developed their phenotype upon ageing. We could observe no difference in phenotype at the juvenile stage, but the two genotypes became distinguishable, after the third week (Figure S6), as reported by Meng *et al.* (2019). Lacking any observable increase in the amounts of RFP-ANAC017 under control conditions in plants of different ages (Figure 7d), the phenotype might correlate with an increased activity of the nuclear localized ANAC017 when plant development proceeds with age. The transcriptional activity of ANAC013 and ANAC017 has been recently shown to be regulated by the nuclear protein RADICAL-INDUCED CELL DEATH1 (RCD1; Shapiguzov *et al.*, 2019), and the relevance of such an interaction might be investigated in the future in the context of flooding stresses.

While the abundance of the N-terminal ANAC017 fragment was equal between juvenile and adult plants (Figure 7d), we observed a difference in the accessibility of its target genes at the chromatin level. Representative ANAC017 target genes were identified among the ARuS genes upon survey of publicly available transcriptomic data (Figure 8a). On their promoters, we could measure enhanced trimethylation of H3K27, a marker of gene repression (Mondal *et al.*, 2016; Pan *et al.*, 2018), in adult plants (Figure 8c). The same genomic regions were characterized by higher DNA methylation (as indicated by low cut/uncut ratio in adult plants; Figure 8a), in line with what has been described for animal models, where DNMT3A1 preferentially methylates cytosines in genomic regions where H3K27me3 marks are present (Manzo *et al.*, 2017). Promotion of a heterochromatic context in specific stress-related genes in adult plants might be interpreted as an adaptive strategy to limit responsiveness, and its high energy costs, in plants destined for reproductive development.

To conclude, in the same genetic background, juvenile Arabidopsis plants showed enhanced survival compared with adult plants under submergence conditions. We showed that this tolerance mechanism is independent of the core-anaerobic response (Figure 3), and rather relies on NAC transcription factors that mediate retrograde stress signalling (Figures 7b and 8). It should be observed that, in this context, ANAC017 anyway contributes positively to plant responses to submergence also at later vegetative stages (Meng *et al.*, 2020). The differential response between developmental stages seems to originate from the chromatin status of the loci targeted by ANAC017, rather than from its direct regulation by the stress. If confirmed in crop species, this finding might help breeding programmes and farming practice to tailor strategies on the specific developmental stage at which submergence-related stresses are experienced.

EXPERIMENTAL PROCEDURES

Plant material and growth conditions

Arabidopsis thaliana Col-0 ecotype was used as wild-type in all the experiments. The T-DNA insertional mutants *anac017-1* (SALK_022174) and *abi2-1* (NASC ID N23), and a *35S:miR156* overexpressing line (N9952; Wang *et al.*, 2009) were obtained from the European Arabidopsis Stock Centre (NASC). Homozygous *anac017-1* plants were confirmed by standard PCR, using the gene-specific primers insANAC017_F (5′-GGGCTCCTAGTGGT GAGCGGACTGA) and insANAC017_R (5′-CTCATCGATATCCTC TAACTGAAGA), and LBb1 (5′-ATTTTGCCGATTTCGGAAC) as a T-DNA specific primer. Plants were germinated and grown on peat (Hawita Flor), using a peat:sand ratio 3:1, after stratification at 4°C in the dark for 48 h. Plants were maintained in a growth chamber under 23°C/18°C (day/night) temperature cycle, 80 μmol photon m^{-2} sec^{-1} light intensity and neutral photoperiod (12 h/12 h light/dark). For axenic growth conditions, seeds were surface-sterilized and germinated on half-strength Murashige and Skoog (Duchefa, Duchefa Biochemie B.V., Haarlem, The Netherlands) basal medium (pH 5.7) supplemented with 5 g L^{-1} sucrose and 8 g L^{-1} plant agar (Duchefa). All experiments entailing the comparison between juvenile and adult plants referred to individuals at the developmental stage defined, respectively, as 1.06 and 1.12 by Boyes (2001), corresponding to 2 and 3 weeks of growth in our experimental conditions.

Submergence experiments and chemical treatments

At end of the light phase, soil-grown plants were submerged with tap water in glass tanks, until the water surface reached approximately 20 cm above the rosettes; water was equilibrated to room temperature along the previous day. Plants were flooded in the dark for the specified duration, while control plants were maintained in darkness in air. After submergence, plants were either sampled for the specific subsequent analyses or moved back to normal photoperiodic conditions and allowed to recover for 1 week before survival scoring. Plants that were able to produce new leaves in the recovery period were categorized as alive, on the opposite they were scored as dead. The number of plants

deployed in each submergence experiment is indicated in the corresponding sections, with a minimum of four replications with 15 plants each. Chemical treatments were administered by spraying with 100 nM antimycin A in 0.001% ethanol 6 h before submergence, or 10 μM ABA in 0.1% ethanol 3 h in advance, whereas control plants were sprayed with the respective solvent.

Microarray analysis

Total RNA was extracted using the Spectrum™ Plant Total RNA Kit (Sigma-Aldrich, Saint Louis, MO, USA) from a pool of three Col-0 plants at the juvenile or adult stage. Two biological replicates were used. Hybridization against the Arabidopsis Gene 1.0 ST Array, washing, staining and scanning were performed by Atlas Biolabs GmbH. Normalization of the raw microarray data and extraction of signal intensities were carried out through the Robust MultiArray methodology (Giorgi *et al.*, 2010). An empirical Bayes method to shrink the probe-wise sample variances was applied to the data, and then differential expression analysis was carried out using the Limma R package (Ritchie *et al.*, 2015).

RNA extraction and real-time qPCR analyses

Equal amounts of total RNA, extracted as above, were subjected to DNase treatment, carried out using the RQ1-DNase kit (Promega), and were reverse transcribed into cDNA using the iScript™ cDNA Synthesis Kit (Bio-Rad, Hercules, CA, USA). Fifteen ng cDNA were used for real-time qPCR amplification with the ABI Prism 7300 sequence detection system (Biosystems), using iQSYBR Green Supermix (Biorad). All primers are listed in Table S1. Relative gene expression was calculated using the $2^{-\Delta\Delta Ct}$ method (Livak and Schmittgen, 2001), based on the housekeeping gene *Ubiquitin10* (*At4g05320*).

Production of RFP-ANAC017-GFP transgenic lines in *Arabidopsis thaliana*

In order to obtain an RFP-ANAC017-GFP fusion construct, the full-length coding sequence of *ANAC017* (1671 bp, devoid of the stop codon) was amplified from an Arabidopsis cDNA sample with the primers gwANAC017_F (5′-CACCATGGCGGATTCTTCACCCGA) and ANAC017-XhoI-HindIII_R (5′-AAGCTTAGAGCTCGAGGTCTTTCAAGAGAAGA). The template was obtained from shoot material extracted as described above, and processed into cDNA by use of RQ1-DNase (Promega, Madison, WI, USA) and SuperScript III Reverse Transcriptase kit (Thermo-Fisher Scientific). The sequence was subsequently cloned in the pENTR/D-TOPO vector (Thermo-Fisher Scientific), to generate a pENTR-ANAC017 plasmid. The GFP coding sequence was amplified from the template plasmid pK7FWG2 (Karimi *et al.*, 2002), with the primers XhoI-eGFP_F (5′-CACCGCGCTCGAGATGGTGAGCAAGGGCGAGG) and eGFP-HindIII_R (5′-CGCAAGCTTTTACTTGTACAGCTCG), and cloned into pENTR to obtain a pENTR-GFP plasmid. Subsequently, the two coding sequences were fused in frame into a new pENTR-ANAC017-GFP vector, upon digestion of the two starting entry plasmids with XhoI and HindIII, and ligation of the resulting pENTR-ANAC017 linearized vector with the GFP fragment. Finally, the Gateway LR clonase II enzyme mix (Thermo-Fisher Scientific, Waltham, MA, USA) was used to recombine pENTR-ANAC017-GFP with the N-terminal tagging vector pUBN-RFP (Grefen *et al.*, 2010). The resulting plant expression vector pUBQ10:RFP-ANAC017-GFP was employed for Arabidopsis stable transformation, achieved through the floral dip method (Zhang *et al.*, 2006). First-generation transformants (T_1) were selected upon germination on MS medium plates containing the herbicide glufosinate-ammonium (PESTANAL®, Sigma-Aldrich). Transgene expression was assessed by real-time qPCR using the primers ANAC017_F and ANAC017_R listed in Table S1. Single-copy transgene insertion was verified by segregation of the T_2 progeny on herbicide-containing plates. Homozygous T_3 or next-generation plants were used for the following experiments.

Western blot

Total protein from shoot tissues of *pUBQ10:RFP-ANAC017-GFP* plants was extracted in a buffer containing 50 mM Tris-HCl pH 7.6, 1 mM EDTA, 100 mM NaCl, 2% sodium dodecyl sulphate (SDS) and 0.05% Tween-20. Fifty micrograms of proteins from the extracts, quantified with the Pierce BCA Protein Assay Kit (Thermo-Fisher Scientific), was separated by SDS–polyacrylamide gel electrophoresis (PAGE) on 10% polyacrylamide Bis-Tris NuPAGE midigels (Thermo-Fisher Scientific) and transferred onto a polyvinylidene difluoride membrane by means of the Trans-Blot Turbo System (Bio-Rad). A monoclonal anti-GFP antibody (Roche, Basel, Switzerland, cat. no. 11814460001) was used at 1:3000 dilution, and combined with a 1:20 000 rabbit anti-mouse secondary antibody (Agrisera, Vännäs, Sweden, cat. no. AS09627) to detect the Δ533ANAC017:GFP protein fragment. A rat monoclonal anti-RFP antibody (Chromotek, ChromoTek GmbH, Planegg, Germany, cat. no. 5F8) was used at 1:1000 dilution and combined with a 1:5000 donkey anti-rat secondary antibody (Agrisera, cat. no. AS10947) to detect the RFP:ANAC017Δ24 protein fragment. All antibodies were diluted in 4% milk in TBS-T. Blots were incubated with the LiteAblot Turbo Extra Sensitive Chemiluminescent Substrate (EuroClone, Milan, Italy) and imaged with UVP VisionWorks LS (Ultra-Violet Products). Equal loading of total protein samples was checked by Amido-black staining of the membrane (Mithran *et al.*, 2014).

ROS staining and quantification

Reactive oxygen species production was visualized in juvenile and adult plants treated in dark submergence conditions for 24 h, starting at the end of the light phase, or sampled before the onset of the treatment. ROS staining and detection was carried out using methods described by Daudi and O'Brien (2012). Briefly, collected plants were stained in freshly prepared 1 mg ml^{-1} DAB (Sigma-Aldrich) neutralized in 10 mM Na_2HPO_4 for 12 h, then chlorophyll was bleached in an ethanol:acetic acid:glycerol = 3:1:1 solution with boiling (95°C for 15 min). After that, plants were imaged by means of an optical scanner, and the acquired images were processed with Image J (Rueden *et al.*, 2017) to obtain a digital quantification of pixel intensity relative to the background and normalized to the area of the object.

ABA quantification

Extraction and determination of ABA content in Arabidopsis shoots were performed as described in Woo *et al.* (2011). Briefly, 200–300 mg plant material was frozen in liquid nitrogen and ground using a Mixer-Mill (Qiagen, Hilden, Germany). The homogenate was extracted with 1–2 ml ABA extraction buffer (10 mM HCl and 1% w/v polyvinyl polypyrrolidone in methanol), with continuous mixing overnight at 4°C. After centrifugation, the supernatant was neutralized with 1 M NaOH, and ABA levels were quantified in the extract using the Phytodetek-ABA kit (AGDIA, Elkhart, Indiana, USA), following the manufacturer's protocol. Raw values for ABA levels were standardized on sample fresh weight and extraction volume.

Genomic DNA methylation analysis

Genomic DNA was extracted from 40 mg leaf material of juvenile or adult *A. thaliana* Col-0 plants kept under control growth conditions, using the Wizard Genomic DNA Purification Kit (Promega). Cytosine

methylation on target loci was assessed by MSRE-qPCR (Hashimoto *et al.*, 2007) using the methylation-sensitive endonucleases HpaII and SalI (Thermo Fisher Scientific). Full information related to target loci identity and location of the target CpG sites evaluated is reported in Table S2. Eight-hundred nanograms of DNA was digested using 1 μl of the respective restriction enzyme (10 U HpaII, or 40 U SalI), or an equal volume of 50% glycerol for mock digestions, in 20 μl reaction volume containing the appropriate buffer according to the manufacturer's recommendations. Reactions were incubated overnight at 37°C, followed by enzyme inactivation at 65°C for 30 min. Enzyme-treated and mock-treated samples were diluted to 10 ng μl^{-1}, and 1 μl DNA was amplified by qPCR using 200 nM of each primer and Power Up SYBR Green Master Mix (Thermo Fisher Scientific). Details on the primers used for the analysis can be found in Table S2. Amplifications were carried out with an ABI Prism 7300 sequence detection system (Applied Biosystems, Watham, MA, USA) with a standard cycling protocol. The methylation level in each sample is expressed as relative amplification level (cut/uncut ratio) between enzyme- and mock-treated DNA, calculated as $2^{-\Delta Ct}$ values, where $\Delta C_t = C_t(cut) - C_t(uncut)$.

Chromatin immunoprecipitation

The extent of histone methylation in juvenile or adult leaf samples was assessed in Col-0 plants by chromatin immunoprecipitation with rabbit polyclonal Anti-Histone H3 (di methyl K4; Abcam, cat. no. ab7766) or Anti-Histone H3 (tri methyl K27) antibody (Abcam, cat. no. ab195477; 5 μg specific antibody added to each sample). Five biological replicates were used, each obtained from 500 mg fresh tissue. The chromatin immunoprecipitation (ChIP) assay was performed according to the protocol described in Giuntoli and Perata (2017). The primers used to specifically quantify genomic DNA abundance by qPCR in immune-purified and input samples are listed in Table S3.

Statistical analyses

All ANOVA and Kaplan–Meier survival analyses were carried out with the aid of the GraphPad Prism version 6.01 for Windows (GraphPad Software, La Jolla, California, USA; http://www.graphpad.com). Additional details related to individual experiments are provided in the corresponding sections and legends.

ACKNOWLEDGEMENTS

This study was funded by Scuola Superiore Sant'Anna, and the Italian Ministry of University and Research (grant no. 20173EWRT9). LTB was financially supported by the PhD programme in Agrobiodiversity of the Scuola Superiore Sant'Anna. The authors thank Prof. Emily Flashman for language reviewing of the manuscript.

AUTHOR CONTRIBUTIONS

FL, LTB and BG designed the experiments. LTB carried out survival analyses, tissue stainings, gene-targeted expression analyses, gene cloning and the production of transgenic plants, in addition to the statistical analyses associated with the above-mentioned experiments. BG carried out immunoblot and MSRE-qPCR analyses. AT quantified ABA levels. FMG analysed the microarray data. VS carried out Chip-PCR analyses. FL and PP secured funding to support the study. FL and BG wrote the manuscript, with inputs by PP. All the authors read and approved the manuscript.

CONFLICT OF INTEREST

The authors declare no conflict of interest.

DATA AVAILABILITY STATEMENT

Microarray data were deposited in the Gene Expression Omnibus repository with the accession number GSE137866.

SUPPORTING INFORMATION

Additional Supporting Information may be found in the online version of this article.

Figure S1. *SPL* family gene expression in juvenile or adult plant.

Figure S2. Regulation of the ARuS genes in response to external perturbations.

Figure S3. Histochemical assessment of ROS production in juvenile and adult plants.

Figure S4. Profile of expression of *ANAC013* (red line), *16* (blue) and *17* (green) across 10 stages of Arabidopsis development.

Figure S5. Expression of three submergence-responsive genes (*CYP71E*, *GST25* and *AOX1D*) in the wild-type and the *anac017-1* mutant.

Figure S6. Phenotypical and molecular evaluation of *pUBQ10:RFP-ANAC017-GFP* transgenic plants.

Figure S7. Full immunoblot images related to Figure 7(d).

Figure S8. DNA methylation at the *UBQ10* and *SPL9* promoters.

Table S1. Primers used for real-time qPCR measurements of gene expression.

Table S2. Primers used for the MSRE-qPCR analysis of the selected genomic loci.

Table S3. Primers used for the ChIP-qPCR assessment of histone 3 methylation on selected ARuS gene loci.

Table S4. Numeric expression values of marker genes for submergence-related processes in treated juvenile ('J.') or adult plants ('A.').

Table S5. Global gene expression analysis in shoot samples from juvenile and adult Col-0 plants after 24 h dark submergence.

Table S6. GO term (biological process) enrichment of the differentially regulated genes under submergence at 2 or 3 weeks of age.

Table S7. Expression profile of ARuS genes in public microarray experiments analysed with the aid of Genevestigator (Hruz *et al.*, 2008).

REFERENCES

Bailey-Serres, J. and Colmer, T.D. (2014) Plant tolerance of flooding stress - recent advances. *Plant Cell Environ.* **37**, 2211–2215.

Bechtold, U. and Field, B. (2018) Molecular mechanisms controlling plant growth during abiotic stress. *J. Exp. Bot.* **69**, 2753–2758.

Benschop, J.J., Jackson, M.B., Gühl, K., Vreeburg, R.A.M., Croker, S.J., Peeters, A.J.M. and Voesenek, L.A.C.J. (2005) Contrasting interactions between ethylene and abscisic acid in Rumex species differing in submergence tolerance. *Plant J.* **44**, 756–768.

Boyes, D.C. (2001) Growth stage-based phenotypic analysis of arabidopsis: a model for high throughput functional genomics in plants. *Plant Cell*, **13**, 1499–1510.

De Clercq, I., Vermeirssen, V., Van Aken, O. *et al.* (2013) The membrane-bound NAC transcription factor ANAC013 functions in mitochondrial retrograde regulation of the oxidative stress response in Arabidopsis. *Plant Cell*, **25**, 3472–3490.

Daudi, A. and O'Brien, J.A. (2012) Detection of hydrogen peroxide by DAB staining in Arabidopsis leaves. *Bio Protoc.* **2**, e263.

Durand, M., Mainson, D., Porcheron, B., Maurousset, L., Lemoine, R. and Pourtau, N. (2018) Carbon source–sink relationship in Arabidopsis thaliana: the role of sucrose transporters. *Planta*, **247**, 587–611.

Gibbs, D.J., Lee, S.C., Md Isa, N. *et al.* (2011) Homeostatic response to hypoxia is regulated by the N-end rule pathway in plants. *Nature*, **479**, 415–418.

Giorgi, F.M., Bolger, A.M., Lohse, M. and Usadel, B. (2010) Algorithm-driven Artifacts in median polish summarization of Microarray data. *BMC Bioinformatics*, **11**, 553.

Giuntoli, B. and Perata, P. (2017) Group VII ethylene response factors in Arabidopsis: regulation and physiological roles. *Plant Physiol.* **176**, 1143–1155.

Gladman, N.P., Marshall, R.S., Lee, K.H. and Vierstra, R.D. (2016) The proteasome stress regulon is controlled by a pair of NAC transcription factors in arabidopsis. *Plant Cell*, **28**, 1279–1296.

Gonzali, S., Loreti, E., Cardarelli, F., Novi, G., Parlanti, S., Pucciariello, C., Bassolino, L., Banti, V., Licausi, F. and Perata, P. (2015) Universal stress protein HRU1 mediates ROS homeostasis under anoxia. *Nat. Plants*, **1**, 15151.

Grefen, C., Donald, N., Hashimoto, K., Kudla, J., Schumacher, K. and Blatt, M.R. (2010) A ubiquitin-10 promoter-based vector set for fluorescent protein tagging facilitates temporal stability and native protein distribution in transient and stable expression studies. *Plant J.* **64**, 355–365.

Hashimoto, K., Kokubun, S., Itoi, E. and Roach, H.I. (2007) Improved quantification of DNA methylation using methylation-sensitive restriction enzymes and real-time PCR. *Epigenetics*, **2**, 86–91.

Hildebrand, F. (1875) Ueber die Jungendzustände solcher Pflanzen, welche im Alter vom vegetativen Charakter ihrer Verwandten abweichen. *Flora*, **21**, 321–330.

Hoffmann-Benning, S. and Kende, H. (1992) On the role of abscisic acid and gibberellin in the regulation of growth in rice. *Plant Physiol.* **99**, 1156–1161.

Hook, D.D., McKee, W.H., Smith, H.K. *et al.* (1988) *Involvement of the hormones ethylene and abscisic acid in some adaptive responses of plants to submergence, soil waterlogging and oxygen shortage. The ecology and management of wetlands*. New York, NY: Springer, pp. 373–382.

Hoson, T., Masuda, Y. and Pilet, P.E. (1993) Abscisic acid content in air- and water-grown rice coleoptiles. *J. Plant Physiol.* **142**, 593–596.

Hruz, T., Laule, O., Szabo, G., Wessendorp, F., Bleuler, S., Oertle, L., Widmayer, P., Gruissem, W. and Zimmermann, P. (2008) Genevestigator V3: a reference expression database for the meta-analysis of transcriptomes. *Adv. Bioinformatics*, **3**, 1–5.

Huijser, P. and Schmid, M. (2011) The control of developmental phase transitions in plants. *Development*, **138**, 4117–4129.

Hurng, W.P., Lur, H.S., Liao, C.K. and Kao, C.H. (1994) Role of abscisic acid, ethylene and polyamines in flooding-promoted senescence of tobacco leaves. *J. Plant Physiol.* **143**, 102–105.

James, S.A. and Bell, D.T. (2001) Leaf morphological and anatomical characteristics of heteroblastic Eucalyptus globulus ssp. Globulus (Myrtaceae). *Aust. J. Bot.* **49**, 259–269.

Kanojia, A. and Dijkwel, P.P.. (2018) Abiotic stress responses are governed by reactive oxygen species and age. *Ann. Plant Rev.* 1–32. https://doi.org/10.1002/9781119312994.apr0611

Karimi, M., Inzé, D. and Depicker, A. (2002) GATEWAY^{TM} vectors for Agrobacterium-mediated plant transformation. *Trends Plant Sci.* **7**, 193–195.

Lee, B., Yu, S. and Jackson, D. (2009) Control of plant architecture: the role of phyllotaxy and plastochron. *J. Plant Biol.* **52**, 277–282.

Lee, S.C., Mustroph, A., Sasidharan, R., Vashisht, D., Pedersen, O., Oosumi, T., Voesenek, L.A.C.J. and Bailey-Serres, J. (2011) Molecular characterization of the submergence response of the *Arabidopsis thaliana* ecotype Columbia. *New Phytol.* **190**, 457–471.

Licausi, F., Kosmacz, M., Weits, D.A., Giuntoli, B., Giorgi, F.M., Voesenek, L.A.C.J., Perata, P. and Van Dongen, J.T. (2011) Oxygen sensing in plants is mediated by an N-end rule pathway for protein destabilization. *Nature*, **479**, 419–422.

Lim, C.C.K., Krebs, S.L. and Arora, R. (2014) Cold hardiness increases with age in juvenile rhododendron populations. *Front. Plant Sci.* **5**, 542.

Liu, Y., Liu, K., Yin, L., Yu, Y., Qi, J., Shen, W.H., Zhu, J., Zhang, Y. and Dong, A. (2019) H3K4me2 functions as a repressive epigenetic mark in plants. *Epigenetics Chromatin*, **12**, 40.

Livak, K.J. and Schmittgen, T.D. (2001) Analysis of relative gene expression data using real-time quantitative PCR and the 2(-Delta Delta C(T)) Method. *Methods*, **25**, 402–408.

Loreti, E., Valeri, M.C., Novi, G. and Perata, P. (2018) Gene regulation and survival under hypoxia requires starch availability and metabolism. *Plant Physiol.* **176**, 1286–1298.

Loreti, E., van Veen, H. and Perata, P. (2016) Plant responses to flooding stress. *Curr. Opin. Plant Biol.* **33**, 64–71.

Manzo, M., Wirz, J., Ambrosi, C., Villaseñor, R., Roschitzki, B. and Baubec, T. (2017) Isoform-specific localization of DNMT3A regulates DNA methylation fidelity at bivalent CpG islands. *EMBO J.* **36**, 3421–3434.

Marias, D.E., Meinzer, F.C. and Still, C. (2017) Impacts of leaf age and heat stress duration on photosynthetic gas exchange and foliar nonstructural carbohydrates in Coffea arabica. *Ecol. Evol.* **7**, 1297–1310.

Matsoukas, I.G., Massiah, A.J. and Thomas, B. (2013) Starch metabolism and antiflorigenic signals modulate the juvenile-to-adult phase transition in Arabidopsis. *Plant Cell Environ.* **36**, 1802–1811.

Meng, X., Li, L., De, C.I. *et al.* (2019) ANAC017 coordinates organellar functions and stress responses by reprogramming retrograde signaling. *Plant Physiol.* **180**, 634–653.

Meng, X., Li, L., Narsai, R., De Clercq, I., Whelan, J. and Berkowitz, O. (2020) Mitochondrial signalling is critical for acclimation and adaptation to flooding in *Arabidopsis thaliana*. *Plant J.* **103**, 227–247.

Mithran, M., Paparelli, E., Novi, G., Perata, P. and Loreti, E. (2014) Analysis of the role of the pyruvate decarboxylase gene family in Arabidopsis thaliana under low-oxygen conditions. *Plant Biol.* **16**, 28–34.

Mondal, S., Go, Y.S., Lee, S.S., Chung, B.Y. and Kim, J.H. (2016) Characterization of histone modifications associated with DNA damage repair genes upon exposure to gamma rays in Arabidopsis seedlings. *J. Radiat. Res.* **57**, 646–654.

Ng, S., Ivanova, A., Duncan, O. *et al.* (2013) A membrane-bound NAC transcription factor, ANAC017, mediates mitochondrial retrograde signaling in Arabidopsis. *Plant Cell*, **25**, 3450–3471.

Pan, M.R., Hsu, M.C., Chen, L.T. and Hung, W.C. (2018) Orchestration of H3K27 methylation: mechanisms and therapeutic implication. *Cell. Mol. Life Sci.* **75**, 209–223.

Poethig, R.S. (2013) Vegetative phase change and shoot maturation in plants. *Curr. Top. Dev. Biol.* **105**, 125–152.

Ritchie, M.E., Phipson, B., Wu, D., Hu, Y., Law, C.W., Shi, W. and Smyth, G.K. (2015) Limma powers differential expression analyses for RNA-sequencing and microarray studies. *Nucleic Acids Res.* **43**, e47.

Rueden, C.T., Schindelin, J., Hiner, M.C., DeZonia, B.E., Walter, A.E., Arena, E.T. and Eliceiri, K.W. (2017) Image J2: ImageJ for the next generation of scientific image data. *BMC Bioinformatics*, **18**, 529.

Saeed, A.I., Sharov, V., White, J. *et al.* (2003) TM4: A free, open-source system for microarray data management and analysis. *Biotechniques*, **34**, 374–378.

Shapiguzov, A., Vainonen, J.P., Hunter, K. *et al.* (2019) Arabidopsis RCD1 coordinates chloroplast and mitochondrial functions through interaction with ANAC transcription factors. *eLife*, **8**, e43284.

Telfer, A., Bollman, K.M. and Poethig, R.S. (1997) Phase change and the regulation of trichome distribution in *Arabidopsis thaliana*. *Development*, **124**, 645–654.

Tsukaya, H., Shoda, K., Kim, G.T. and Uchimiya, H. (2000) Heteroblasty in *Arabidopsis thaliana* (L.) Heynh. *Planta*, **210**, 536–542.

van Dongen, J.T. and Licausi, F. (2015) Oxygen sensing and signaling. *Annu. Rev. Plant Biol.* **66**, 345–346.

Voesenek, L.A.C.J. and Bailey-Serres, J. (2015) Flood adaptive traits and processes: an overview. *New Phytol.* **206**, 57–73.

Wang, J.W., Czech, B. and Weigel, D. (2009) miR156-Regulated SPL transcription factors define an endogenous flowering pathway in *Arabidopsis thaliana*. *Cell*, **138**, 738–749.

Weits, D.A., Giuntoli, B., Kosmacz, M., Parlanti, S., Hubberten, H.M., Riegler, H., Hoefgen, R., Perata, P., Van Dongen, J.T. and Licausi, F. (2014) Plant cysteine oxidases control the oxygen-dependent branch of the N-end-rule pathway. *Nat. Commun.* **5**, 3425.

White, M.D., Klecker, M., Hopkinson, R.J. *et al.* (2017) Plant cysteine oxidases are dioxygenases that directly enable arginyl transferase-catalysed arginylation of N-end rule targets. *Nat. Commun.* **8**, 14690.

Wingler, A. (2018) Transitioning to the next phase: the role of sugar signaling throughout the plant life cycle. *Plant Physiol.* **176**, 1075–1084.

Woo, D.-H., Park, H.-Y., Kang, I.S., Lee, S.-Y., Moon, B.Y., Lee, C.B. and Moon, Y.-H. (2011) Arabidopsis lenc1 mutant displays reduced ABA

accumulation by low AtNCED3 expression under osmotic stress. *J. Plant Physiol.* **168**, 140–147.

Wu, G., YeonPark, M., Conway, S.R., Wang, J.W., Weigel, D. and Poethig, R.S. (2009) The Sequential Action of miR156 and miR172 Regulates Developmental Timing in Arabidopsis. *Cell*, **138**(4), 750–759. https://doi.org/10.1016/j.cell.2009.06.031

Xu, M., Hu, T., Zhao, J., Park, M.-Y., Earley, K.W., Wu, G., Yang, L. and Poethig, R.S. (2016) Developmental functions of miR156-regulated SQUAMOSA PROMOTER BINDING PROTEIN-LIKE (SPL) genes in *Arabidopsis thaliana*. *PLoS Genet.* **12**, e1006263.

Yeung, E., Bailey-Serres, J. and Sasidharan, R. (2019) After the deluge: plant revival post-flooding. *Trends Plant Sci.* **24**, 443–454.

Yeung, E., van Veen, H., Vashisht, D. *et al.* (2018) A stress recovery signaling network for enhanced flooding tolerance in *Arabidopsis thaliana*. *Proc. Natl Acad. Sci. USA*, **115**, E6085–E6094.

Yu, S., Li, C., Zhou, C.M., Zhang, T.Q., Lian, H., Sun, Y., Wu, J., Huang, J., Wang, G. and Wang, J.W. (2013) Sugar is an endogenous cue for juvenile-to-adult phase transition in plants. *eLife*, **2**, e00269.

Zhang, X., Henriques, R., Lin, S.-S., Niu, Q.-W. and Chua, N.-H. (2006) Agrobacterium-mediated transformation of Arabidopsis thaliana using the floral dip method. *Nat. Protoc.* **1**, 641–646.

Zhang, L., Hu, Y.B., Sen, W.H., Feng, S.J. and Zhang, Y.T. (2015) Involvement of miR156 in the regulation of vegetative phase change in plants. *J. Am. Soc. Hortic. Sci.* **140**, 387–395.